Ramakrishna Mission Residential College (Autonomous)

Kolkata 700103, WB, India

Collaborative research in coordination chemistry of organic radicals

Number 11

Institute 1: Ramakrishna Mission Residential College (Autonomous)

Concerned Faculty: Dr. Prasanta Ghosh, Dept of Chemistry

&

Institute 2: Max-Planck-Institut für Chemische Energiekonversion

Stiftstrasse 34 - 36 / D - 45470 Mülheim an der Ruhr

Concerned Scientist: Dr Thomas Weyhermüller

Period of Investigation: 20-01-2016 to 15-10-2016

Project: Anion radical complexes of oxidovanadium(IV)

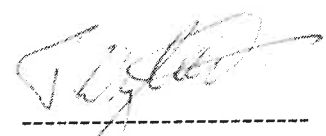**Output:** The result was published in a journal of international repute

Publication: Coordination of o-benzosemiquinonate, o-iminobenzosemiquinonate, 4,4'-di-tert-butyl-2,2'-bipyridine and 1,10-phenanthroline anion radicals to oxidovanadium(IV)

Madhusudan Shit, Suvendu Maity, Sachinath Bera, Thomas Weyhermüller and Prasanta Ghosh*

New J. Chem, 2016, *40*, 10305-10315

Dr. Prasanta Ghosh

Dr Thomas Weyhermüller

ROYAL SOCIETY
OF CHEMISTRY

PAPER

CrossMark
click for updates

Coordination of o-benzosemiquinonate, o-iminobenzosemiquinonate, 4,4′-di-tert-butyl-2,2′-bipyridine and 1,10-phenanthroline anion radicals to oxidovanadium(IV)†

Madhusudan Shit,[a] Suvendu Maity,[a] Sachinath Bera,[a] Thomas Weyhermüller[b] and Prasanta Ghosh*[a]

This article reports on the stabilization of organic radical anions promoted by the oxidovanadium(IV) ion. A 3,5-di-tert-butylcatecholate (^{tBu}catH$^-$) complex of oxidovanadium(V) of the type [(L$^a_{ONO}$$^{2-}$)(VO^{3+})(^{tBu}catH$^-$)] (1) was isolated using tridentate (E)-N′-((3-hydroxynaphthalen-2-yl)methylene)benzohydrazide (L$^a_{ONO}$H$_2$) as a coligand, whereas o-benzosemiquinonate (sq$^{\bullet-}$) and p-nitro-o-iminobenzosemiquinonate (^{NO2}isq$^{\bullet-}$) radical anion complexes of oxidovanadium(IV) of the types [(L$_{NNO}$$^-$)(VO^{2+})(sq$^{\bullet-}$)] (2) and [(L$_{NNO}$$^-$)(VO^{2+})(^{NO2}isq$^{\bullet-}$)] (3) were successfully isolated using (1Z,N′E)-N′-(phenyl(pyridin-2-yl)methylene)benzohydrazonic acid (L$_{NNO}$H) as a coligand. Oxidovanadium(IV) complexes of the types [(L$^b_{ONO}$$^{2-}$)(VO^{2+})(phen)] (4) and [(L$^b_{ONO}$$^{2-}$)(VO^{2+})(^{tBu}bpy)] (5), which undergo reversible reduction to the 4,4′-di-tert-butyl-2,2′-bipyridine radical anion (^{tBu}bpy$^{\bullet-}$) and the 1,10-phenanthroline radical anion (phen$^{\bullet-}$) to afford the coupled states [(L$^b_{ONO}$$^{2-}$)(VO^{2+})(phen$^{\bullet-}$)]$^-$ (4$^-$) and [(L$^b_{ONO}$$^{2-}$)(VO^{2+})(^{tBu}bpy$^{\bullet-}$)]$^-$ (5$^-$), respectively, were isolated (L$^b_{ONO}$H$_2$ = (E)-N′-(2-hydroxybenzylidene)benzohydrazide). The molecular geometries of the complexes were confirmed by the single-crystal X-ray structure determinations of 1, 3 and 4. In 1, the V–O$_{phenolato}$ length cis to V=O is 1.879(2) Å and the dissimilar V–O and V–OH lengths corresponding to the ^{tBu}catH$^-$ ligand are 1.832(2) and 2.312(2) Å, respectively. In 1, the average C–O lengths in ^{tBu}catH$^-$ are 1.351(3) Å, whereas in 3 the average C–O and C–N lengths in ^{NO2}isq$^{\bullet-}$ are 1.293(4) and 1.355(5) Å, respectively. In 4, the V–O$_{phenolato}$ length cis to V=O (1.937(3) Å) is relatively longer. The ^{51}V NMR spectrum of 1 displays a signal at −337.2 ppm, whereas the signals for 2 and 3 are deshielded to +382.4 and +71.8 ppm, respectively. The closed-shell singlet (CSS) solutions of 3 and 5$^-$ at the B3LYP/DFT level are unstable and the open-shell singlet (OSS) solutions are 0.5 and 7.3 kcal mol^{-1} lower in energy, respectively, than the CSS solutions. In 3 and 5$^-$ the alpha spin (100%) is localized on the vanadium ion, whereas the beta spin is delocalized across the aminophenol and bipyridine fragments. 2 and 3 exhibit lower-energy absorption bands at 785 and 585 nm, which are defined as CSS → OSS perturbation transitions.

Introduction

Chemists have been interested in organic radicals since 1900.[1] From a fundamental perspective and for the investigation of new activities, the characterization of organic radicals that enable several important reactions in chemistry is worthwhile.[2] The participation of radical intermediates in biology and catalytic

[a] Department of Chemistry, R. K. Mission Residential College, Narendrapur, Kolkata-103, India. E-mail: ghosh@pghosh.in
[b] Max-Planck-Institut für Chemische Energiekonversion, Stiftstrasse 34-36, D-45470 Mülheim, Germany

† Electronic supplementary information (ESI) available: X-ray geometry of 5 and the gas-phase optimized coordinates of 3, 5, 5$^+$ and 5$^-$. CCDC 1489208, 1489210 and 1508431. For ESI and crystallographic data in CIF or other electronic format see DOI: 10.1039/c6nj02220k

cycles has been disclosed in many cases.[3] Recent studies reveal that the coordination of organic radicals expands the range of activity of the central metal ion.[4] Thus, the detection of organic radicals in the laboratory is a subject of topical interest. Organic radicals are short-lived species and their isolation is a challenge in experimental research. The stabilization of such radicals in coordination complexes of transition metal ions has been successful in the laboratory and various types of transition metal complexes containing organic radicals have been reported.[5] The coordination of reactive organic radicals to transition metal ions is successfully detected in solution in many cases.[6]

The participation of vanadium in several biological redox reactions has provided an impetus to the faster growth of oxidovanadium chemistry in the laboratory.[7] However, the coordination chemistry of organic radicals with oxidovanadium

ions has lacked the proper attention. Only a few oxidovanadium complexes of organic radicals have been reported so far.[8] The isolation of coordination complexes of oxidovanadium ions (VO^{n+}) that contain organic radicals is a part of our ongoing research program.[9] The VO^{3+} state of the redox-active VO^{n+} ion is diamagnetic, whereas the VO^{2+} state is paramagnetic. Recently, it was disclosed that the VO^{2+} ion is an agent that can stabilize organic radicals in complexes.[9] Oxidovanadium(IV) complexes of the o-benzosemiquinonate and o-iminobenzosemiquinonate radical anions were successfully isolated, but surprisingly no organic radical complex of the VO^{3+} ion has been documented. Moreover, no radical anion complexes of oxidovanadium ions other than those of o/p-benzosemiquinonate and o-iminobenzosemiquinonate have been reported so far. In this study, in addition to new complexes of the 3,5-di-$tert$-butylcatecholate (^{tBu}catH$^-$), o-benzosemiquinonate (sq$^{\bullet-}$) and p-nitro-o-iminobenzosemiquinonate (^{NO2}isq$^{\bullet-}$) radical anions, which were isolated as crystalline materials, the coordination of the heterocyclic α-diimines like 4,4′-di-$tert$-butyl-2,2′-bipyridine and 1,10-phenanthroline radical anions ^{tBu}bpy$^{\bullet-}$ and phen$^{\bullet-}$ to oxidovanadium(IV) was successfully detected.

The oxidovanadium(IV/V) complexes $[(L^a{}_{ONO}{}^{2-})(VO^{3+})(^{tBu}catH^-)]$ (1), $[(L_{NNO}{}^-)(VO^{2+})(sq^{\bullet-})]$ (2), $[(L_{NNO}{}^-)(VO^{2+})(^{NO2}isq^{\bullet-})]$ (3), $[(L^b{}_{ONO}{}^{2-})(VO^{2+})(phen)]$ (4) and $[(L^b{}_{ONO}{}^{2-})(VO^{2+})(^{tBu}bpy)]$ (5) isolated in this work are summarized in Chart 1 ($L^a{}_{ONO}H_2$ = (E)-N'-((3-hydroxynaphthalen-2-yl)methylene)benzohydrazide, $L^b{}_{ONO}H_2$ = (E)-N'-(2-hydroxybenzylidene)benzohydrazide and $L_{NNO}H$ = (E)-N'-(phenyl(pyridin-2-yl)methylene)benzohydrazide).

In this article, the syntheses and molecular and electronic structures of 1–5 are reported. 1–5 were characterized by IR, mass, UV-vis, ^{1}H and ^{51}V NMR and EPR spectra and cyclic voltammetry, including single-crystal X-ray diffraction studies of 1, 3 and 4. 2^-, 4^+, 4^-, 5^+ and 5^- were generated by constant-potential coulometric experiments. The coordination of phen$^{\bullet-}$ and ^{tBu}bpy$^{\bullet-}$ to the oxidovanadium(IV) ion in 4^- and 5^- was investigated by spectroelectrochemical measurements and density functional theory (DFT) calculations.

Experimental section

Materials and methods

3,5-Di-$tert$-butylcatechol (^{tBu}catH$_2$), p-nitro-o-aminophenol (^{NO2}apH$_2$), 1,10-phenanthroline (phen) and 4,4′-di-$tert$-butyl-2,2′-bipyridine (^{tBu}bpy) were purchased from Sigma-Aldrich, and other reagents or analytical-grade materials were obtained from commercial suppliers and were used without further purification. Spectroscopic-grade solvents were used for spectroscopic and electrochemical measurements. The synthetic precursors $VO(acac)_2$, (E)-N'-((3-hydroxynaphthalen-2-yl)methylene)benzohydrazide ($L^a{}_{ONO}H_2$), (E)-N'-(2-hydroxy benzylidene)benzohydrazide ($L^b{}_{ONO}H_2$) and (1Z,N′E)-N'-(phenyl(pyridin-2-yl)methylene)benzohydrazonic acid ($L_{NNO}H$) were prepared by reported procedures.[10] The C, H, and N contents of the compounds were determined using a PerkinElmer 2400 Series II elemental analyzer. The elemental analyses were performed after evaporating solvents under high vacuum. Infrared spectra of samples were recorded from 4000 to 400 cm^{-1} with KBr pellets at 295 K using a PerkinElmer Spectrum RX 1 Fourier transform infrared (FT-IR) spectrophotometer. ^{1}H and ^{51}V NMR spectra were recorded in CDCl$_3$ with a Bruker DPX 500 MHz spectrometer. Electrospray ionization (ESI) mass spectra were recorded using a micro mass Q-TOF mass spectrometer. Electronic absorption spectra of solutions of the complexes were recorded with a PerkinElmer Lambda 750 spectrophotometer in the range of 3300–175 nm. X-band EPR spectra were recorded using a Magnettech GmbH MiniScope MS400 spectrometer (equipped with a TC H03 temperature controller), where the microwave frequency was measured with an FC400 frequency counter. The EPR spectra were simulated using EasySpin software. A BASi Epsilon-EC electroanalytical instrument was used for cyclic voltammetric experiments in CH$_2$Cl$_2$ containing 0.2 M tetrabutylammonium hexafluorophosphate as the supporting electrolyte. A BASi platinum working electrode, a platinum auxiliary electrode, and a Ag/AgCl reference electrode were used for the measurements. The redox potential data were referenced to those of the ferrocenium/ferrocene (Fc$^+$/Fc) couple. A BASi SEC-C thin-layer quartz glass spectroelectrochemical cell kit (light path length of 1 mm) with a platinum gauze working electrode and an SEC-C platinum counter electrode were used for spectroelectrochemistry measurements.

Syntheses

$[(L^a{}_{ONO}{}^{2-})(VO^{3+})(^{tBu}catH^-)]$ (1). To (E)-N'-((3-hydroxynaphthalen-2-yl)methylene)benzohydrazide ($L^a{}_{ONO}H_2$) (292 mg, 1 mmol) in a round-bottom flask, MeOH (20 mL) was added and the resulting

Chart 1 Isolated complexes of oxidovanadium(IV/V).

mixture was heated at 325 K for 5 min, then cooled to RT and filtered. To this solution, solutions of VO(acac)$_2$ (262 mg, 1.0 mmol) in CH$_2$Cl$_2$ (2 mL) and methanol (5 mL) followed by 3,5-di-*tert*-butylcatechol (^{tBu}catH$_2$, 222.0 mg, 1.0 mmol) in MeOH (5 mL) were added. The reaction mixture was allowed to evaporate slowly in air. After 2–3 days, crystals of **1** separated out, which were collected by filtration and dried in air. Yield: 240 mg ($\sim$42% with respect to vanadium). Mass spectral data [electrospray ionization (ESI), positive ion, CH$_3$OH]: *m/z* 576 for [**1**]$^+$. Anal. calcd for C$_{32}$H$_{33}$N$_2$O$_5$V: C, 66.66; H, 5.77; N, 4.86; found: C, 66.12; H, 5.72; N, 4.83. ^{1}H NMR (DMSO-d6, 300 MHz, 295 K): δ 10.8 (–OH), 9.88 (s, 1H), 9.50 (s, 1H), 8.92 (d, 1H), 8.52 (d, 1H), 8.15 (t, 2H), 7.92–7.47 (m, 3H), 7.22 (d, 1H), 7.26 (d, 1H), 7.19 (s, 1H), 6.96 (s, 1H), 6.14 (s, 1H), 1.50 (s, 9H), 1.32 (s, 9H) ppm. IR/cm^{-1} (KBr): ν 3430(br), 2958(m), 2926(m), 2853(m), 1603(s), 1548(m), 1516(m), 1495(m), 1467(m), 1448(m), 1405(m), 1382(m), 1285(m), 990(s), 980(m).

[(L$_{NNO}$$^-$)(VO^{2+})(sq$^{•-}$)] (2). To (*E*)-*N'*-(phenyl(pyridin-2-yl)-methylene)benzohydrazide (L$_{NNO}$H) (300 mg, 1 mmol) in a round-bottom flask, MeOH (20 mL) was added and the resulting mixture was heated at 325 K for 5 min, then cooled to RT and finally filtered. To this solution, solutions of VO(acac)$_2$ (262 mg, 1.0 mmol) in CH$_2$Cl$_2$ (2 mL) and methanol (5 mL) followed by catechol (110.04 mg, 1.0 mmol) in acetonitrile (5 mL) were added. The reaction mixture was allowed to evaporate slowly in air. After 2–3 days, red crystals of **2** separated out, which were collected by filtration and dried in air. Yield: 340 mg ($\sim$71% with respect to vanadium). Mass spectral data [electrospray ionization (ESI), positive ion, CH$_3$OH]: *m/z* 498 for [**2** + Na]$^+$. Anal. calcd for C$_{25}$H$_{20}$N$_3$O$_4$V: C, 62.90; H, 4.22; N, 8.80; found: C, 62.67; H, 4.20; N, 8.75. ^{1}H NMR (CDCl$_3$, 300 MHz, 295 K): δ 8.25 (d, 1H), 8.06 (d, 2H), 7.91 (t, 1H), 7.81 (d, 1H), 7.62–7.58 (m, 4H), 7.47–7.41 (m, 3H), 7.30 (t, 2H), 6.64 (br, 4H) ppm. IR/cm^{-1} (KBr): ν 1502(m), 1489(m), 1460(s), 1424(s), 1371(s), 1337(m), 1322(m), 1302(m), 1258(s), 1140(s), 1079(s), 954(s), 710(s), 690(s).

[(L$_{NNO}$$^-$)(VO^{2+})(^{NO2}isq$^{•-}$)] (3). To (*E*)-*N'*-(phenyl(pyridin-2-yl)-methylene)benzohydrazide (L$_{NNO}$H) (300 mg, 1 mmol) in a round-bottom flask, MeOH (20 mL) was added and the resulting mixture was heated at 325 K for 5 min, then cooled to RT and filtered. To this solution, solutions of VO(acac)$_2$ (262 mg, 1.0 mmol) in CH$_2$Cl$_2$ (2 mL) and MeOH (5 mL) followed by *p*-nitro-*o*-aminophenol (^{NO2}AP, 154.0 mg, 1.0 mmol) in aceto-nitrile (5 mL) were added. The reaction mixture was allowed to evaporate slowly in air. After 2–3 days, green crystals of **3** separated out, which were collected by filtration and dried in air. Yield: 390 mg ($\sim$75% with respect to vanadium). Mass spectral data [electrospray ionization (ESI), positive ion, CH$_3$OH]: *m/z* 520 for [**3**]$^+$. Anal. calcd for C$_{25}$H$_{18}$N$_5$O$_5$V: C, 57.81; H, 3.49; N, 13.48; found: C, 57.57; H, 3.48; N, 13.43. ^{1}H NMR (CDCl$_3$, 300 MHz, 295 K): δ 14.83 (s, 1H), 8.25 (d, 1H), 8.08 (d, 2H), 8.03 (t, 1H), 7.98 (t, 3H), 7.61 (d, 4H), 7.44–7.22 (m, 5H), 6.47 (d, 1H) ppm. IR/cm^{-1} (KBr): ν 3252(br), 1564(s), 1579(s), 1503(s), 1488(s), 1461(s), 1428(s), 1363(m), 1318(s), 1249(m), 1076(s), 965(s), 947(m), 704(m), 691(m).

[(L^b$_{ONO}$$^{2-}$)(VO^{2+})(phen)] (4). To (*E*)-*N'*-(2-hydroxybenzylidene)-benzohydrazide (L^b$_{ONO}$H$_2$) (240 mg, 1 mmol) in a round-bottom

flask, MeOH (20 mL) was added and the resulting mixture was heated at 325 K for 5 min, then cooled to RT and filtered. To this solution, solutions of VO(acac)$_2$ (262 mg, 1.0 mmol) in CH$_2$Cl$_2$ (2 mL) and methanol (5 mL) followed by 1,10-phenanthroline (phen, 180 mg, 1.0 mmol) in MeOH (5 mL) were added. The reaction mixture was allowed to evaporate slowly in air. After 2–3 days, red crystals of **4** separated out, which were collected by filtration and dried in air. Yield: 380 mg ($\sim$78% with respect to vanadium). Mass spectral data [electrospray ionization (ESI), positive ion, CH$_3$OH]: *m/z* 486 for [**4** + H]$^+$. Anal. calcd for C$_{26}$H$_{18}$N$_4$O$_3$V: C, 64.34; H, 3.74; N, 11.54; found: C, 64.03; H, 3.73; N, 11.50. IR/cm^{-1} (KBr): ν 1609(m), 1591(m), 1540(m), 1510(s), 1492(m), 1469(m), 1442(m), 1419(m), 1350(s), 1149(m), 963(m), 955(s), 848(m), 726(m), 705(m).

[(L^b$_{ONO}$$^{2-}$)(VO^{2+})(^{tBu}bpy)] (5). To (*E*)-*N'*-(2-hydroxybenzylidene)-benzohydrazide (L^b$_{ONO}$H$_2$) (240 mg, 1 mmol) in a round-bottom flask, MeOH (20 mL) was added and the resulting mixture was heated at 325 K for 5 min, then cooled to RT and filtered. To this solution, solutions of VO(acac)$_2$ (262 mg, 1.0 mmol) in CH$_2$Cl$_2$ (2 mL) and methanol (5 mL) followed by 4,4'-di-*tert*-butyl-2,2'-bipyridine (^{tBu}bpy, 268.00 mg, 1.0 mmol) in MeOH (5 mL) were added. The reaction mixture was allowed to evaporate slowly in air. After 2–3 days, red crystals of **5** separated out, which were collected by filtration and dried in air. Yield: 395 mg ($\sim$69% with respect to vanadium). Mass spectral data [electrospray ionization (ESI), positive ion, CH$_3$OH]: *m/z* 574 for [**5** + H]$^+$. Anal. calcd for C$_{32}$H$_{34}$N$_4$O$_3$V: C, 67.01; H, 5.97; N, 9.77; found: C, 66.83; H, 5.94; N, 9.73. IR/cm^{-1} (KBr): ν 2965(br), 1610(s), 1539(m), 1513(m), 1494(m), 1468(m), 1444(m), 1406(m), 1357(m), 1149(m), 1037(m), 951(s), 899(m), 703(m).

[(L$_{NNO}$$^-$)(VO^{2+})(cat^{2-})]$^-$ (2$^-$), **[(L^b$_{ONO}$$^{2-}$)(VO^{3+})(phen)]$^+$ (4$^+$)**, **[(L^b$_{ONO}$$^{2-}$)(VO^{2+})(phen$^{•-}$)]$^-$ (4$^-$)**, **[(L^b$_{ONO}$$^{2-}$)(VO^{3+})(^{tBu}bpy)]$^+$ (5$^+$)** and **[(L^b$_{ONO}$$^{2-}$)(VO^{2+})(^{tBu}bpy$^{•-}$)]$^-$ (5$^-$)**. These complexes were not isolated but were generated by constant-potential coulo-metric experiments in CH$_2$Cl$_2$ at 296 K for spectroelectro-chemical measurements and EPR spectroscopy. 2$^-$, 4$^-$ and 5$^-$ were generated by the reduction of **2**, **4** and **5**, respectively, at –1.00, –2.40, and 2.50 V with respect to the Fc$^+$/Fc couple, whereas 4$^+$ and 5$^+$ were produced by the oxidation of **4** and **5**, respectively, at +1.0 and +0.05 V.

Single-crystal X-ray structure determination (CCDC no. 1489208, 1489210 and 1508431)

Dark single crystals of **1**, **3** and **4** were picked up with nylon loops and mounted on a Bruker AXS D8 QUEST ECO diffracto-meter equipped with a Mo target rotating-anode X-ray source and a graphite monochromator (Mo Kα, λ = 0.71073 Å). Final cell constants were obtained from least-squares fits of all measured reflections. Intensity data were corrected for absorp-tion using intensities of redundant reflections. The structures were readily solved by direct methods and subsequent difference Fourier techniques. The Siemens SHELXS-97[20a] software package was used for solution, SHELXL-97[20b] was used for refinement and XS. Ver. 2013/1,[20c] XT. Ver. 2014/4[20d] and XL. Ver. 2014/7[20e] were used for structure solution and refinement. All non-hydrogen atoms were refined anisotropically. Hydrogen atoms were placed

at the calculated positions and refined as riding atoms with isotropic displacement parameters.

A split-atom model was also used to account for the severe disorder of both ligands in 1. Part of the naphthyl unit in 1 containing atoms C13, C14, and C19–C22 was split into two positions, giving occupation factors of 0.66 and 0.34, respectively. The EADP, ISOR, SAME and SADI instructions were used to restrain parts. The two t-butyl groups were split into two (C37–C40) and three orientations (C33–C36), giving occupation ratios of about 0.745 : 0.255 and 0.46 : 0.35 : 0.19, respectively. The EADP, SADI, and ISOR restraints were employed. Platon/ SQUEEZE[20f,g] was used to remove residual density peaks (max. 3.2 e Å^{-3}) of a highly disordered unknown solvent molecule. The volume of the void was calculated to be about 340 Å^3.

A split-atom model was also used to account for disorder in the crystal of compound 3. A phenyl ring (C57–C62), which was found to be disordered by rotation, was treated as explained above. The occupation ratio of the two parts was refined to a value of about 0.77 : 0.23 in this case. The nitro group N33–O35 attached to C29 was also split into two slightly skewed positions. The occupation factors were refined to values of about 0.53 and 0.47. Some minor residual density peaks (below 1.9 e Å^{-3}) were detected in a void with a volume of about 100 Å^3. It is very likely that these density peaks originated from the solvent of crystallization (probably CH$_3$OH, which was used with CH$_2$Cl$_2$ to grow single crystals for X-ray diffraction studies), which almost completely evaporated from the crystal before or at the time of data collection. Platon/SQUEEZE[20f,g] was used to remove these peaks from the refinement.

Density functional theory (DFT) calculations

All calculations reported in this article were performed with the Gaussian 03W[21] program package supported by GaussView 4.1. The DFT[22] and time-dependent (TD) DFT[23] calculations were performed at the level of the Becke three-parameter hybrid functional with the nonlocal correlation functional of Lee–Yang–Parr (B3LYP).[24] The gas-phase geometries of 3, 5$^+$ and 5$^-$ were optimized in the singlet spin state, whereas 5 was optimized in the doublet spin state, using Pulay's direct inversion[25] in the iterative subspace (DIIS) "tight" convergent self-consistent field procedure[26] ignoring symmetry. All the calculations were performed with the LANL2DZ basis set,[27] with the corresponding effective core potential (ECP) for vanadium, the 6-31+G*(d,p)[28] basis set for C, O, and N atoms, and 6-31G[29] for H atoms. The closed-shell singlet (CSS) solutions of 3 and 5$^-$ are unstable. In both cases, the energies of the corresponding open-shell singlet (OSS) solutions, which are stable, are lower than those of the CSS solutions. The 60 lowest singlet excitation energies for each of the optimized geometries of 3 and 5$^-$ were determined by TD DFT calculations.

Results and discussion

Syntheses and characterization

(E)-N'-(2-Hydroxybenzylidene)benzohydrazide (L^b$_{ONO}$H$_2$) and (E)-N'-(phenyl(pyridin-2-yl)methylene)benzohydrazide (L$_{NNO}$H)

were prepared by the reported procedures.[10] L^a$_{ONO}$H$_2$ was prepared by following the synthetic procedure of L^b$_{ONO}$H$_2$. The reaction of VO(acac)$_2$ with L^a$_{ONO}$H$_2$ and 3,5-di-$tert$-butyl-catechol (^{tBu}catH$_2$) in MeOH afforded 1, where the VO^{2+} ion was oxidized to the VO^{3+} ion in air. The similar reaction with catechol (cat) and L$_{NNO}$H produced 2, where cat was oxidized to sq$^{•-}$. However, in the presence of triethylamine, ^{tBu}catH$^-$ in 1 underwent deprotonation and reduced the VO^{3+} ion, which yielded an EPR-silent [(L^a$_{ONO}$$^{2-}$)(VO^{2+})(^{tBu}sq$^{•-}$)]$^-$ (1a) state. The reaction of VO(acac)$_2$ with L$_{NNO}$H and p-nitro-o-aminophenol (^{NO2}ap) promoted the oxidation of ^{NO2}ap to ^{NO2}isq$^{•-}$ in air, which generated 3. The reactions of VO(acac)$_2$ with L^b$_{ONO}$H$_2$ and 4,4′-di-$tert$-butyl-2,2′-bipyridine (^{tBu}bpy) and 1,10-phenanthroline (phen) yielded 4 and 5. Details of the syntheses are outlined in the experimental section. The IR spectrum of 1 displayed a broad absorption band at 3430 cm^{-1} due to aromatic –OH functions, which was absent in 2. The peak due to the N–H stretching vibration of 3 appeared at 3252 cm^{-1}. The peak due to the V^V=O stretching vibration of 1 was observed at 990 cm^{-1}, whereas those of the V^{IV}=O stretching vibrations of 2–5 appeared at 955 ± 10 cm^{-1}, and the trend correlates well with those reported in the literature.[9]

Electrochemical studies and EPR spectroscopy

The redox activities of 1–5 were investigated by cyclic voltammetry in CH$_2$Cl$_2$ at 295 K and the redox potential data referenced to those of the ferrocenium/ferrocene (Fc$^+$/Fc) couple are summarized in Table 1. The cyclic voltammograms are illustrated in Fig. 1.

Both the cathodic and anodic waves of 1 are irreversible. The cathodic wave of 2 at −0.78 V, which is assigned to the sq$^{•-}$/cat^{2-} redox couple, is reversible, whereas the anodic peak due to the q/sq$^{•-}$ couple at +0.74 V is irreversible. The cyclic voltammogram of 3 is different from that of 2. Both the cathodic and anodic peaks of 3 at −0.97 V and +1.39 V, which are due to the isq$^{•-}$/ap^{2-} and iq/isq$^{•-}$ redox couples, respectively, are irreversible (q = o-benzoquinone, iq = o-iminobenzoquinone; ap^{2-} = o-amidophenolato). The cyclic voltammograms of 4 and 5 are illustrated in Fig. 1(d and e), respectively. 4 exhibits one reversible anodic wave at −0.09 V owing to the VO^{3+}/VO^{2+} redox couple, whereas the equivalent redox wave of 5 appears at −0.16 V. The VO^{3+}/VO^{2+} redox waves of 4 and 5 are similar to those reported in cases of [V^{IV}O(L)(bpy)] and [V^{IV}O(L)(phen)] complexes,[11] where L is an ONO donor dianionic tridentate ligand. No redox waves of [V^{IV}O(L)(bpy)] and [V^{IV}O(L)(phen)]

Table 1 Redox potential data referenced to the Fc$^+$/Fc couple determined by cyclic voltammetry in CH$_2$Cl$_2$ (0.20 M [N(n-Bu)$_4$]PF$_6$) at 295 K

Compound	$E_{1/2}^1$ (V) (ΔE^a, mV)	$E_{1/2}^2$ (V) (ΔE^a, mV)
1	+0.12^b	−1.23^c
2	+0.74	−0.78 (155)
3	+1.39	−0.97
4	−0.09 (140)	−2.16 (175)
5	−0.16 (140)	−2.23 (190)

^{a} Peak-to-peak separation in mV. ^{b} Anodic peak. ^{c} Cathodic peak.
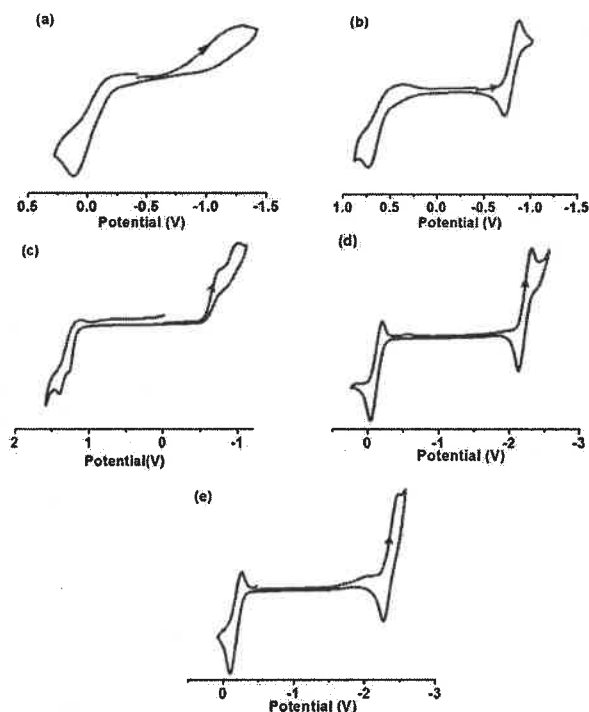
Fig. 1 Cyclic voltammograms of (a) **1**, (b) **2**, (c) **3**, (d) **4** and (e) **5** in CH$_2$Cl$_2$ (0.20 M [N(n-Bu)$_4$]PF$_6$) at 295 K.

Fig. 2 X-band EPR spectra of (a) **4**, (b) **5** and (c) **2**$^-$ in CH$_2$Cl$_2$ at 295 K (black, experimental; red, simulated).

Table 2 X-band EPR spectral parameters of **4**, **5** and **2**$^-$ ions in CH$_2$Cl$_2$ at 295 K

Complex	g	A (G)	lw
4	1.965	80 (^{51}V, $I = 7/2$)	2.1
5	1.964	80 (^{51}V, $I = 7/2$)	2.2
2$^-$	1.965	92 (^{51}V, $I = 7/2$)	3

complexes at the cathode were successfully detected. However, **4** and **5** display reversible cathodic waves at −2.16 and −2.23 V, respectively, which are assigned to the phen/phen$^{•-}$ and ^{tBu}bpy/^{tBu}bpy$^{•-}$ redox couples. The corresponding cathodic wave of the 2,2′-bipyridine (unsubstituted) analogue [(L$_{ONO}$$^{2-}$)(VO^{2+})(bpy)] is not quite reversible ($\Delta E > 250$ mV) and this complex is not included in this report. The coordination of phen$^{•-}$ and ^{tBu}bpy$^{•-}$ to the oxidovanadium(IV) ion is unprecedented and the origin of its formation is attributed to the higher anti-ferromagnetic coupling constant between two paramagnetic centers (see below).

The fluid-solution EPR spectra of **4** and **5** are illustrated in Fig. 2(a and b), respectively. The EPR spectral parameters are listed in Table 2. The spectra exhibit hyperfine splitting due to ^{51}V nuclei ($I = 7/2$). The g-parameters obtained from simulations of the EPR spectra are 1.965 and 1.964, respectively. The EPR spectrum of **2**$^-$ is similar to those of **4** and **5**, as shown in Fig. 2(c), which confirms that **2**$^-$ is an oxidovanadium(IV) complex of the type [(L$_{NNO}$$^-$)(VO^{2+})(^{tBu}cat^{2-})]$^-$ (**2**$^-$).

Assignment of the electronic states of the complexes

In conjunction with the EPR spectroscopy, X-ray bond parameters, ^{51}V NMR spectroscopy and density functional theory (DFT) calculations were used to confirm the electronic states of the complexes.

X-ray crystallography

The crystallographic data of **1**, **3** and **4** are summarized in Table 3. **1** crystallizes in the $P2_1/c$ space group. The molecular
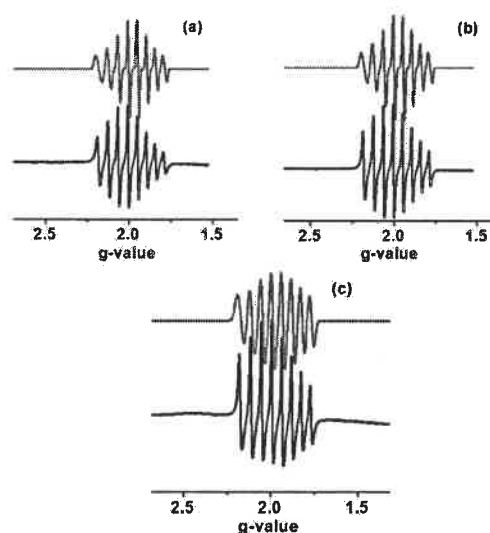
Table 3 Crystallographic data for **1**, **3** and **4**

CCDC no.	1 (1508431)	3 (1489210)	4 (1489208)
Formula	C$_{32}$H$_{33}$N$_2$O$_5$V	C$_{25}$H$_{18}$N$_5$O$_5$V	C$_{26}$H$_{18}$N$_4$O$_3$V
f_w	576.54	519.38	485.38
Crystal system	Monoclinic	Orthorhombic	Monoclinic
Crystal color	Black	Green	Red
Space group	$P2_1/c$	$P2_12_12_1$	$C2/c$
a (Å)	11.1788(5)	13.8584(5)	21.5463(13)
b (Å)	18.3320(9)	16.1145(6)	8.3435(5)
c (Å)	17.6872(8)	22.9607(9)	25.3092(15)
α (deg)	90	90	90
β (deg)	107.635(2)	90	107.290(2)
γ (deg)	90	90	90
V (Å)	3454.3(3)	5127.6(3)	4344.3(5)
Z	4	8	8
T (K)	293(2)	293(2)	293(2)
2θ	54.98	54.00	63.9
ρ calcd (g cm^{-3})	1.109	1.346	1.484
Refl. collected	49527	78927	30617
Unique refl.	7878	11180	6679
Reflections ($I > 2\sigma(I)$)	6245	8993	5386
$F(000)$	1208	2128	1992
No. of params/restr.	423/431	654/124	308/0
λ (Å)/μ (mm^{-1})	0.71073/0.323	0.71073/0.430	0.71073/0.495
R1^a [$I > 2\sigma(I)$]/GOF^b	0.0637/1.033	0.0403/1.037	0.0857/1.242
wR2^c [$I > 2\sigma(I)$]	0.1727	0.0859	0.1745
Residual density (e Å^{-3})	0.396	0.229	0.554

^{a} $R1 = \sum ||F_o| - |F_c||/\sum|F_o|$. ^{b} GOF $= \{\sum[w(F_o^2 - F_c^2)^2]/(n - p)\}^{1/2}$. ^{c} wR2 $= \{\sum[w(F_o^2 - F_c^2)^2]/\sum[w(F_o^2)^2]\}^{1/2}$ where w $= 1/[\sigma^2(F_o^2) + (aP)^2 + bP]$, $P = (F_o^2 + 2F_c^2)/3$.

structure of **1** in crystals and the atom labelling scheme are illustrated in Fig. 3(a). Selected bond parameters are summarized
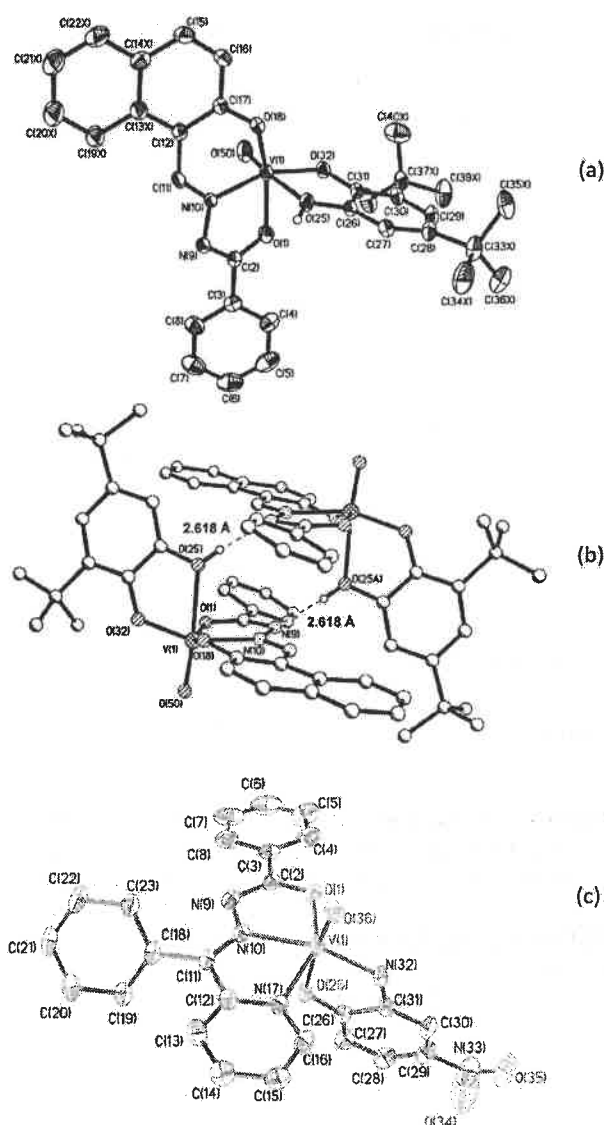
(a)

(b)

(c)

Fig. 3 Molecular geometries of (a) 1 (disordered atoms refined by the split-atom model have been labelled with an X), (b) dimeric 1 and (c) 3 in crystals (30% thermal ellipsoids; H atoms are omitted for clarity).

Table 4 Selected experimental bond lengths (Å) in 1 and 3 and calculated bond lengths (Å) in 3

Bond	1 Exp.	3 Exp.	3 Calc. CSS	3 Calc. BS(↓↑) S = 0
V=O_{oxido}	1.582(2)	1.593(3)/1.596(2)	1.586	1.586
V(1)–O(1), V–$O_{benzoyl}$	1.972(2)	1.980(3)/1.977(2)	1.962	1.993
V(1)–N(10), V–N_{imine}	2.072(2)	2.083(3)/2.091(3)	2.120	2.067
V(1)–N(17), V–$N_{pyridine}$		2.114(3)/2.122(3)	2.129	2.162
V(1)–O(18), V–$O_{phenolato}$	1.879(2)			
V(1)–O(25), V–OH_{cat}	2.312(2)			
V(1)–O(25), V–O_{isq}		2.144(3)/2.106(3)	2.164	2.271
V(1)–N(32), V–N_{isq}		1.895(3)/1.903(3)	1.879	2.114
V(1)–O(32), V–O_{cat}	1.832(2)			
O(1)–C(2)	1.284(3)	1.287(4)/1.300(4)	1.295	1.293
C(2)–N(9)	1.311(3)	1.318(5)/1.316(5)	1.334	1.340
N(9)–N(10)	1.398(3)	1.380(4)/1.376(4)	1.349	1.350
N(10)–C(11)	1.292(3)	1.295(5)/1.292(5)	1.305	1.306
O(25)–C(26)	1.355(3)	1.299(4)/1.286(4)	1.291	1.270
C(31)–O(32)	1.346(3)			
C(31)–N(32)		1.359(5)/1.351(4)	1.373	1.331
C(26)–C(31)	1.400(4)	1.419(5)/1.427(5)	1.440	1.478
C(26)–C(27)	1.387(4)	1.405(5)/1.400(5)	1.420	1.431
C(27)–C(28)	1.395(4)	1.366(6)/1.382(6)	1.383	1.375
C(28)–C(29)	1.395(4)	1.383(7)/1.392(6)	1.413	1.424
C(29)–C(30)	1.393(4)	1.380(6)/1.369(5)	1.394	1.381
C(30)–C(31)	1.407(3)	1.404(5)/1.392(5)	1.397	1.422

in Table 4. $L^a_{ONO}{}^{2-}$ is a tridentate dianionic ligand and coordinates to the oxidovanadium(v) ion meridionally. Both the $L^a_{ONO}{}^{2-}$ and $^{tBu}catH_2$ ligands are severely disordered and a split-atom model, as stated in the experimental section, was used to refine the structure. The bond lengths are approximately close to those in the Ph–C(O⁻)=N–N=CH–Ar–O⁻ resonance state of the ligand. The V–$O_{benzoyl}$ and V–N_{imine} lengths are 1.972(2) and 2.072(2) Å, respectively. The V=O (1.582(2) Å) and V–$O_{phenolato}$ (1.879(2) Å) bonds cis to V=O are relatively shorter and correlate well with those of VO³⁺ complexes.[12] The catechol and o-aminophenol ligands can generate versatile electronic states with oxidovanadium ions.[8,9] The two V–O bonds corresponding to the ^{tBu}cat ligand in 1 are significantly different. The V–O(32) (cis to V=O) length is 1.832(2) Å, whereas, because of the stronger σ-effect of the oxido bond, the V–O(25) bond (2.312(2) Å) trans to V=O is

relatively longer. The bond parameters of the $^{tBu}catH^-$ ligand are similar to those of the oxidovanadium(v) complexes containing mono-deprotonated catechol and 3,5-di-tert-butyl-catechol ligands reported by Chakravorty et al.[13] In these complexes, the two C–O lengths (averages) are 1.364(4) and 1.350(5) Å, respectively. In 1, the corresponding lengths are O(25)–C(26), 1.355(3) Å and O(32)–C(31), 1.346(3) Å. No quinoidal distortion of the C–C lengths in the aromatic ring in 1 was recorded. In 1, the OH (O25) functional group exhibits strong H-bonding with the imine nitrogen (N9) of an adjacent molecule and promotes dimerization, as illustrated in Fig. 3b.

3 crystallizes in the $P2_12_12_1$ space group. The molecular geometry of 3 in crystals and the atom labelling scheme are depicted in Fig. 3(c). The unit cell contains two independent molecules, of which the bond parameters that are not the same are listed in Table 4. The Ph–C(O⁻)=N–N=CH–pyridine state of the tridentate monoanionic ligand $L_{NNO}{}^-$ coordinates to the vanadium(IV) ion in a meridional fashion. The V–$O_{benzoyl}$ and V–N_{imine} lengths are 1.980(3) and 2.083(3) Å, respectively. The V–$N_{pyridine}$ length is 2.114(3) Å, whereas the V=O length is 1.593(3) Å. It is notable that the V–$O_{benzoyl}$ and V=O lengths in 3 are relatively longer than those in 1, owing to the VO²⁺ state in 3. The bond parameters of the redox-active aminophenol ligand are significant for analyzing the electronic state of 3. The average C–O and C–N lengths in the chelate, which are 1.293(4) and 1.355(5) Å, respectively, are relatively shorter and correlate well with those reported in o-iminobenzosemiquinonate radical anion complexes of oxidovanadium(IV).[9] The C–C lengths in the aromatic ring exhibit quinoidal distortion, by which the C27–C28 and C29–C30 lengths are relatively shorter (see Table 4). These features correspond to the $^{NO2}isq^{•-}$ state of the coordinated aminophenol ligand in 3. Characteristically, the average V–N_{isq} length of 1.899(3) Å in 3
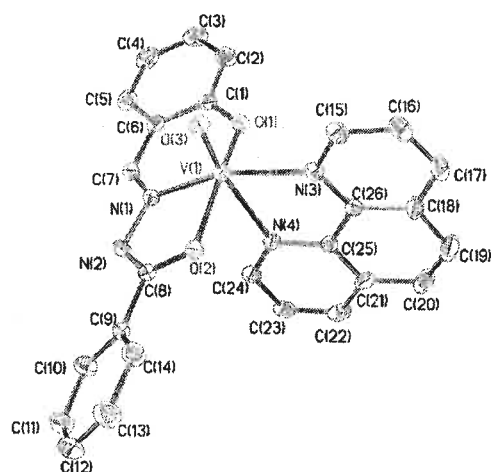
Fig. 4 Molecular geometry of **4** in crystals (40% thermal ellipsoids; H atoms are omitted for clarity).

is relatively shorter than that observed in other *o*-iminobenzo-semiquinonate radical anion complexes of oxidovanadium(ɪᴠ), whereas the average V–O$_{isq}$ bond (2.115(3) Å) *trans* to V=O is relatively longer.

4 crystallizes in the *C*2/*c* space group. The molecular geometry of **4** in crystals and the atom labelling scheme are shown in Fig. 4. Selected bond lengths are listed in Table 5. The resonance state of the L$_{ONO}^-$ ligand is Ph–C(O$^-$)=N–N=CH–sal(O$^-$), as was observed in the case of **1**. The V–O$_{benzoyl}$ and V–N$_{imine}$ lengths in **4** are 2.014(3) and 2.047(3) Å, respectively. The trend in the V–O$_{benzoyl}$ lengths is as follows: **4** > **3** > **1**. The V=O length in **4** is 1.602(3) Å. The V–O$_{phenolato}$ bond *cis* to V=O (1.937(3) Å) is relatively longer than that in **1** and correlates well with those in oxidovanadium(ɪᴠ) complexes. The two V–N$_{phen}$ lengths in **4** differ significantly: the V–N$_{phenyl}$ bond (2.351(3) Å) *trans* to V=O is relatively longer than the V–N$_{phenyl}$ bond (2.155(3) Å) *trans* to V–N$_{imine}$ and the C$_{py}$–C$_{py}$ length is 1.429(5) Å.

5 crystallizes in the *C*2/*c* space group,[14] but the diffraction data are not satisfactory because R_{int} > 0.10. However, we were

successful in refining the structure and the gross geometry is similar to that of **4**, as shown in Fig. S1 (ESI†). The bond parameters obtained from the single-crystal X-ray diffraction study of **5** were not further used for analysis.

^{51}V NMR spectroscopy

The ^{51}V NMR spectra of **1–3** were recorded in CDCl$_3$ and the spectra of **2** and **3** are shown in Fig. 5. It was established that the ^{51}V resonance signal of oxidovanadium(ɪᴠ) coupled to an organic radical is significantly deshielded.[15] The ^{51}V resonance signal of **1**, which contains oxidovanadium(ᴠ), appears at δ = −337.23 ppm and correlates well with those reported in cases of oxidovanadium(ᴠ) catecholato complexes.[13] In contrast, the ^{51}V chemical shift of **2** is deshielded to δ = +382.4 ppm. This feature is similar to those of oxidovanadium(ɪᴠ) complexes that contain *o*-benzosemiquinonate radical anions.[9] Similarly, the ^{51}V signal of **3** is deshielded to δ = +71.8 ppm, which correlates with those of *o*-iminobenzosemiquinonate radical anion complexes of oxidovanadium(ɪᴠ). The chemical shifts of the ^{51}V nucleus imply that **1** is an oxidovanadium(ᴠ) complex of catecholate, whereas **2** and **3** are complexes of oxidovanadium(ɪᴠ) coupled to organic radicals.

DFT calculations

DFT calculations were employed on **3**, **5**, **5$^+$** and **5$^-$** to determine the electronic structures of the complexes and their oxidized
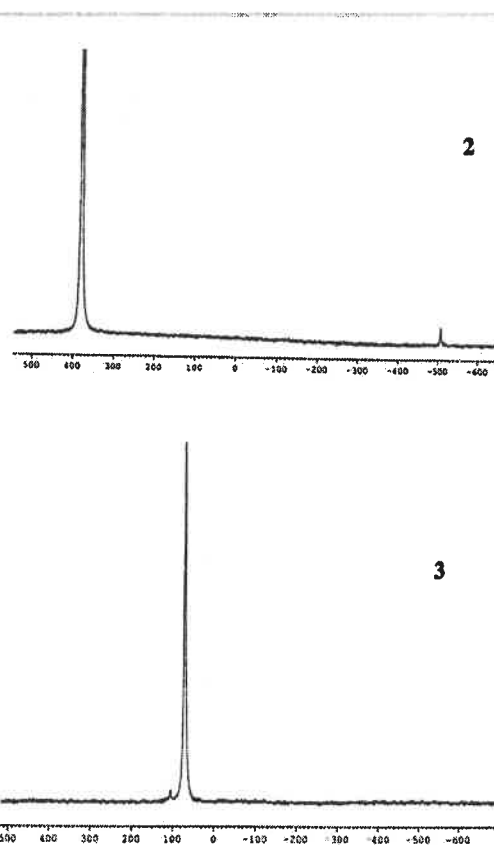
Table 5 Selected experimental bond lengths (Å) in **4** and calculated bond lengths (Å) in **5**, **5$^+$** and **5$^-$**

Bond	4 Exp.	5 Calc.	5$^+$ Calc.	5$^-$ Calc.
V(1)–O(1), V–O$_{phenolato}$	1.937(3)	1.944	1.819	2.015
V(1)–O(2), V–O$_{benzoyl}$	2.014(3)	1.995	1.886	2.048
V(1)–N(1), V–N$_{imine}$	2.047(3)	2.058	2.093	2.119
V(1)–N(3), V–N$_{phen}$	2.155(3)	2.218	2.176	2.013
V(1)–N(4), V–N$_{phen}$	2.351(3)	2.412	2.298	2.327
V(1)–O(3), V=O	1.602(3)	1.591	1.575	1.602
C(1)–O(1)	1.320(4)	1.313	1.344	1.295
N(1)–C(7)	1.291(4)	1.303	1.306	1.302
N(1)–N(2)	1.408(4)	1.386	1.368	1.385
N(2)–C(8)	1.310(4)	1.319	1.307	1.322
O(2)–C(8)	1.300(4)	1.305	1.328	1.290
N(3)–C(26)	1.364(4)	1.353	1.357	1.390
C(25)–C(26)	1.429(5)	1.486	1.480	1.444
N(4)–C(25)	1.351(4)	1.344	1.348	1.363

Fig. 5 ^{51}V NMR spectra of **2** and **3** in CDCl$_3$.

and reduced analogues. The gas-phase geometry of **3** was optimized in singlet and triplet spin states. Analysis of the stability of the solution confirmed that the closed-shell singlet (CSS) solution of **3** is unstable owing to the open-shell singlet (OSS) perturbation, and this was further reoptimized in the OSS state. The OSS solution, which has 60% diradical character, is 0.5 kcal mol^{-1} lower in energy than the CSS solution. The triplet solution is 1.6 kcal mol^{-1} higher in energy than the CSS solution. However, the broken-symmetry (BS) ↑↓ state of **3** is only 0.6 kcal mol^{-1} higher in energy than the CSS state (↑ denotes an unpaired spin-up electron on fragment **1** and ↓ denotes an unpaired spin-down electron essentially localized on fragment **2**). The optimized bond parameters of the CSS and BS (↓↑) states are summarized in Table 4. The calculated V=O, V–O$_{benzoyl}$, V–N$_{imine}$ and V–N$_{pyridine}$ lengths in **3** correlate well with those obtained from the single-crystal X-ray diffraction study of **3**. The calculated shorter C–O (1.291 Å) and C–N (1.373 Å) lengths and the quinoidal distortion of the C–C lengths of the coordinated *o*-aminophenol ligand correspond well to those of coordinated *o*-iminobenzosemiquinonate radical anions.[16] The C–O and C–N lengths obtained from the BS (↓↑) calculation are relatively shorter (see Table 4). Moreover, the localization of the alpha spin on the vanadium ion and the beta spin on the *o*-aminophenol fragment, as depicted in Fig. 6(a), revealed by the BS(↓↑) solution confirms a major contribution of the diradical singlet state to the ground electronic state of **3**, which is defined as a ^{NO2}isq$^{•-}$ complex of oxidovanadium(IV). In **3**, the atomic spin is predominantly localized on the nitrogen atom (41%), which results in stronger anti-ferromagnetic coupling with the VO^{2+} ion, and the V–N$_{isq}$ length of 1.879 Å (exp, 1.896(4) Å) is relatively shorter.

The calculated bond parameters of **5** in the doublet state are similar to those found for the single-crystal X-ray structure of **4**, in which the atomic spin is predominantly localized on the vanadium ion, which corresponds to the oxidovanadium(IV)
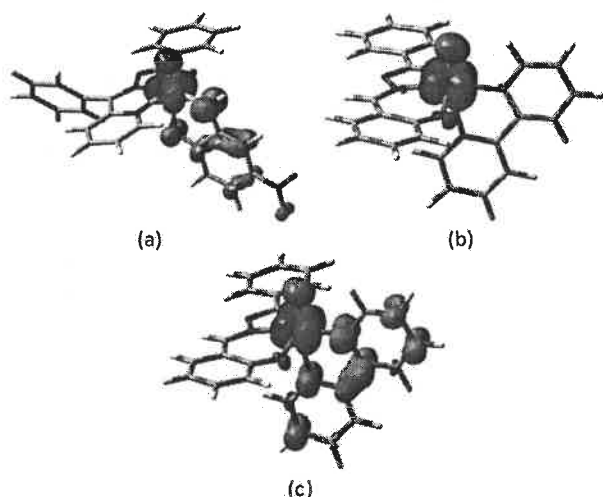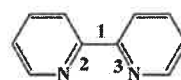

Fig. 6 Atomic spins of (a) **3** (V, 1.15; N32, −0.41; O25, −0.13; C31, −0.17; C30, −0.14; O36, −0.14; C26, −0.08), (b) **5** and (c) **5**$^-$ (V, 1.04; N3, −0.19; N4, −0.17; C16, −0.12; C17, −0.15; C23, −0.16; C25, −0.03; C26, −0.24) obtained from Mulliken spin population analyses.

complex	bonds (Å)		
	1	**2**	**3**
	(C$_{py}$–C$_{py}$)	(C–N)	(C–N)
5	1.486	1.344	1.353
5$^+$	1.480	1.348	1.357
5$^-$	1.444	1.363	1.389

Chart 2 Calculated bond lengths in the 2,2′-bipyridine fragment of **5**, **5**$^+$ and **5**$^-$.

state. However, the calculated V=O, V–O$_{phenolato}$, V–O$_{benzoyl}$ and V–N$_{imine}$ lengths in the **5**$^+$ ion in the singlet spin state are relatively shorter than those in **5**; in particular, the shorter V–O$_{phenolato}$ bond (1.819 Å) *cis* to V=O is a marker of the oxidovanadium(V) state.[12,17] This implies that the **5**$^+$ ion is an oxidovanadium(V) complex of the type [(L$_{ONO}$$^{2-}$)(VO^{3+})(bpy)]$^+$.

In contrast, the calculated V–O$_{phenolato}$, V–O$_{benzoyl}$ and V–N$_{imine}$ lengths in the **5**$^-$ ion in the singlet spin state are relatively longer than those in **5**. Moreover, the CSS solution of the **5**$^-$ ion is unstable owing to OSS perturbation. It was observed that the OSS solution of the **5**$^-$ ion with 100% diradical character is lower in energy than the CSS solution by 7.3 kcal mol^{-1}. In the **5**$^-$ ion the alpha spin is localized on the vanadium ion (1.04), whereas the beta spin is delocalized on the bpy fragment, as depicted in Fig. 6(c). It is notable that the triplet state of **5**$^-$ is also 5.2 kcal mol^{-1} lower in energy than the singlet state. The bond parameters of the bpy fragment of **5**$^-$ obtained for the CSS and triplet states are significantly different from those of **5** and the **5**$^+$ ion, as stated in Chart 2.

The C$_{py}$–C$_{py}$ length of 1.444 Å in **5**$^-$ is relatively shorter than those (average C$_{py}$–C$_{py}$ = 1.483 Å) in **5** and **5**$^+$, whereas the average C–N lengths of 1.376 Å are relatively longer. Notably, this feature is consistent with those observed in bpy$^{•-}$ complexes of alkali and transition metal ions.[18] Thus, the **5**$^-$ ion is defined as a bpy$^{•-}$ complex of the oxidovanadium(IV) ion of the type [(L$_{ONO}$$^{2-}$)(VO^{2+})(bpy$^{•-}$)]$^-$. The coupling constant (*J*) was calculated using the Yamaguchi approach.[19] The value of *J*$_{cal}$ is −750 cm^{-1} and the coupling scheme is (VO^{2+})↑(bpy$^{•-}$)↓. It is predicted that the higher exchange energy due to coupling of the unpaired electrons of the oxidovanadium(IV) ion and bpy$^{•-}$ and phen$^{•-}$ radical anions is an important factor in the coordination of these reactive radical anions to the paramagnetic oxidovanadium(IV) ion in the **4**$^-$ and **5**$^-$ ions.

Electronic spectra

The UV-vis/NIR absorption spectra of L$_{ONO}$H$_2$ and complexes **1–5** were recorded in CH$_2$Cl$_2$ at 295 K and the spectra are illustrated in Fig. 7. The free ligand L^b$_{ONO}$H$_2$ absorbs strongly at 327 nm owing to a π → π* transition. In addition to a band at 330 nm, a band at around 400 nm appears for all complexes owing to this transition. The electronic spectrum of **1** displays a band at 580 nm (ε = 0.10) owing to ^{tBu}catH$^-$ → VO^{3+} charge transfer (LMCT type). The electronic spectrum of **2** displays an absorption maximum at 785 nm, which is absent in that of **1**.
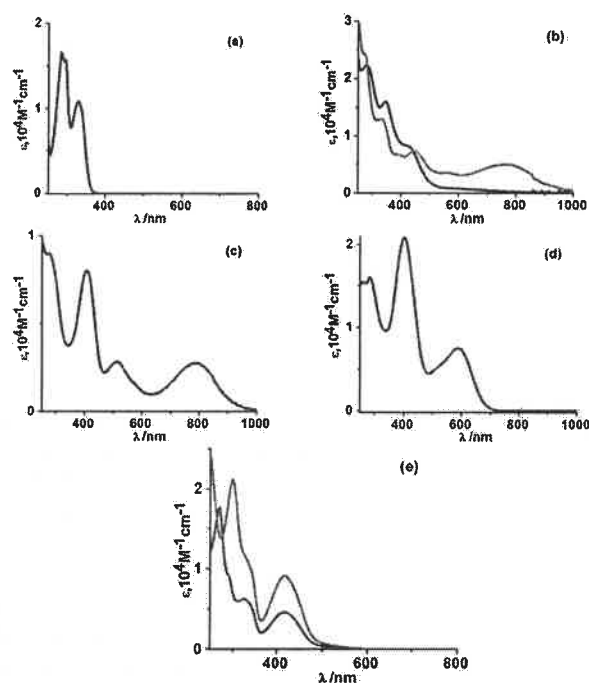
This journal is © The Royal Society of Chemistry and the Centre National de la Recherche Scientifique 2016

Fig. 7 UV-vis/NIR absorption spectra of (a) $L_{ONO}H_2$, (b) **1** (black), **1a** (red), (c) **2**, (d) **3**, (e) **4** (blue), and **5** (pink) in CH_2Cl_2 at 295 K.

Fig. 8 Changes in UV-vis/NIR absorption spectra during the conversions of (a) **2 → 2⁺**, (b) **4 → 4⁺**, (c) **4 → 4⁻**, (d) **5 → 5⁺** and (e) **5 → 5⁻** recorded by spectroelectrochemical measurements.

Table 6 Electronic spectral data of **1–5**, **1a**, **4⁺**, **5⁺**, **2⁻**, **4⁻** and **5⁻** in CH_2Cl_2 at 295 K

Complex	λ_{max} (nm) (ε, 10^4 M^{-1} cm^{-1})
1	580 (0.10), 420 (0.83), 345 (1.60), 280 (2.24)
1a	770 (0.52), 450 (0.75), 390 (0.68), 330 (1.30), 275 (2.43)
2	785 (0.27), 515 (0.28), 407 (0.80), 280 (0.90)
2⁻	785 (0.11), 515 (0.13), 405 (0.37), 290 (0.99)
3	585 (0.75), 400 (2.10), 285 (1.60)
4	415 (0.42), 325 (0.63), 270 (1.7)
4⁺	410 (0.31), 320 (0.76), 290 (1.12)
4⁻	425 (0.17), 315 (0.83), 290 (1.24), 270 (1.88)
5	415 (0.92), 330 (1.12), 300 (2.12)
5⁺	410 (0.62), 330 (1.23), 290 (2.30)
5⁻	400 (0.34), 330 (1.12), 290 (3.23)

The electronic spectrum of **2** corresponds well to those of oxidovanadium(ɪv) complexes of *o*-benzosemiquinonate radical anion complexes reported recently.[8,9] DFT calculations on the singlet state of **2** were performed to determine the excitation energies in MeOH. The value of λ_{cal} is 692.9 nm (f = 0.05) owing to dioxolene → vanadium (LMCT) and dioxolene → L_{ONN}^- (ILCT) transitions. ILCT is the origin of λ_{cal} at 678.3 nm (f = 0.03). The former transition of **2** is assigned to CSS → OSS perturbation transitions (LMCT type), where the CSS solution is unstable (Table 6).

A violet solution of **1** in CH_2Cl_2 upon the addition of triethylamine turned blue, which indicated a bathochromic shift in the absorption maximum. The electronic spectrum of this solution was recorded and is illustrated in Fig. 7(b). This spectrum is similar to that of **2** (Fig. 7c), with a lower-energy absorption maximum at 770 nm. Analyses predict that in the
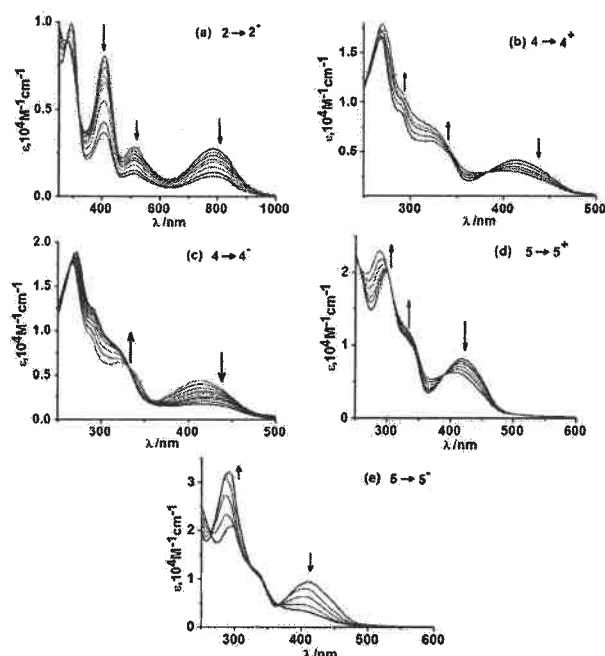
presence of triethylamine ^{tBu}catH⁻ is deprotonated to ^{tBu}cat²⁻, which reduces oxidovanadium(v) to oxidovanadium(ɪv) and is itself oxidized to the ^{tBu}sq•⁻ state, affording an EPR-silent coupled state. This implies that in the presence of a base and air **1** undergoes a facile conversion to a ^{tBu}sq•⁻ complex of the type $[(L_{ONO}^{2-})(VO^{2+})(^{tBu}sq•^-)]^-$ (**1a**), which displays a CSS → OSS transition at 770 nm and is isoelectronic to **2**.

The electronic spectrum of **3** displays a lower-energy absorption band at 585 nm (Fig. 7(d)). The corresponding values of λ_{cal} obtained from TD DFT calculations on **3** in CH_2Cl_2, which are due to AP → L_{ONN}^- (ILCT) and AP → vanadium (LMCT) transitions, are 579.1 and 537 nm. These features are similar to those of **2**, **1a** and reported oxidovanadium(ɪv) complexes that contain an *o*-iminobenzosemiquinonate radical anion.[8,9]

4 and **5** exhibit characteristic bands at 415 nm (Fig. 7(e)), the origin of which is LLCT. As expected, the intensity of the maxima of these bands sharply decreased upon reduction to phen•⁻ and bpy•⁻ radical anions, as depicted in Fig. 8(c and e). In comparison, the conversions of **4 → 4⁺** and **5 → 5⁺** blueshifted the maxima of the bands at 410 nm, as illustrated in Fig. 8(b and d).

Conclusions

This article discloses the coordination of *o*-benzosemiquinonate (sq•⁻), *o*-iminobenzosemiquinonate (isq•⁻), 1,10-phenanthroline (phen•⁻) and 4,4′-di-*tert*-butyl-2,2′-bipyridine (^{tBu}bpy•⁻) radical anions to an oxidovanadium(ɪv) ion. Oxidovanadium complexes of the types $[(L^a_{ONO}^{2-})(VO^{3+})(^{tBu}catH^-)]$ (**1**), $[(L_{NNO}^-)(VO^{2+})(sq•^-)]$

(2), $[(L_{NNO}^{-})(VO^{2+})(^{NO2}isq^{•-})]$ (3), $[(L^{b}_{ONO}^{2-})(VO^{2+})(phen)]$ (4) and $[(L^{b}_{ONO}^{2-})(VO^{2+})(^{tBu}bpy)]$ (5) $(L^{a}_{ONO}^{2-}, L^{b}_{ONO}^{2-}$ and L_{NNO}^{-} are tridentate ligands) were isolated. In the presence of triethylamine and air, 1, which is a catecholato complex of oxidovanadium(v), affords an $sq^{•-}$ complex of oxidovanadium(ɪv) of the type $[(L^{a}_{ONO}^{2-})(VO^{2+})(^{tBu}sq^{•-})]^{-}$ (1a). 4 and 5 undergo reversible reduction to give $phen^{•-}$ and $^{tBu}bpy^{•-}$ complexes of the types $[(L^{b}_{ONO}^{2-})(VO^{2+})(phen^{•-})]^{-}$ (4⁻) and $[(L^{b}_{ONO}^{2-})(VO^{2+})(^{tBu}bpy^{•-})]^{-}$ (5⁻). The ^{51}V resonance signals of 2 and 3 are sharply different from that of 1. In 2 and 3 the signals are deshielded to +382.4 and +71.8 ppm, respectively, whereas the signal is shielded to −357.5 ppm in 1. DFT calculations confirmed that the closed-shell singlet solutions (CSS) of 3 and 5⁻ are unstable. The open-shell singlet (OSS) solutions of 3 and 5⁻ with diradical character are lower in energy than the corresponding CSS solutions. It was established that the larger anti-ferromagnetic coupling constants between oxidovanadium(ɪv) and $phen^{•-}/^{tBu}bpy^{•-}$ are the driving force of the coordination of these reactive radical anions to the paramagnetic oxidovanadium(ɪv) ion.

Acknowledgements

Notes and references

1 M. Gomberg, *J. Am. Chem. Soc.*, 1900, **22**, 757.

2 (a) I. Pappas, S. Treacy and P. J. Chirik, *ACS Catal.*, 2016, **6**, 4105–4109; (b) M. E. O'Reilly and A. S. Veige, *Chem. Soc. Rev.*, 2014, **43**, 6325–6369; (c) O. R. Luca and R. H. Crabtree, *Chem. Soc. Rev.*, 2013, **42**, 1440–1459; (d) V. Lyaskovskyy and B. de Bruin, *ACS Catal.*, 2012, **2**, 270–279; (e) R. G. Hicks, *Nat. Chem.*, 2011, **3**, 189–191; (f) P. Chirik and K. Wieghardt, *Science*, 2010, **327**, 794–795.

3 J. A. Stubbe and W. A. van der Donk, *Chem. Rev.*, 1998, **98**, 705–762.

4 D. L. J. Broere, R. Plessius and J. I. Vlugt, *Chem. Soc. Rev.*, 2015, **44**, 6886–6915.

5 (a) I. S. Morgan, A. Mansikkamäki, G. A. Zissimou, P. A. Koutentis, M. RouziÀres, R. Clérac and H. M. Tuononen, *Chem. – Eur. J.*, 2015, **21**, 15843–15853; (b) W. Kaim and B. Schwederski, *Coord. Chem. Rev.*, 2010, **254**, 1580–1588; (c) A. I. Poddel'sky, V. K. Cherkasov and G. A. Abakumov, *Coord. Chem. Rev.*, 2009, **253**, 291–324; (d) E. Bill, E. Bothe, P. Chaudhuri, K. Chlopek, D. Herebian, S. Kokatam, K. Ray, T. Weyhermüller, F. Neese and K. Wieghardt, *Chem. – Eur. J.*, 2005, **11**, 204–224; (e) C. G. Pierpont, *Coord. Chem. Rev.*, 2001, **219-221**, 415–433.

6 (a) A. Kochem, G. Gellon, O. Jarjayes, C. Philouze, N. Leconte, M. van Gastel, E. Bill and F. Thomas, *Chem. Commun.*, 2014, **50**, 4924–4926; (b) C. T. Lyons and T. D. P. Stack, *Coord. Chem.*

Rev., 2013, **257**, 528–540; (c) T. Büttner, J. Geier, G. Frison, J. Harmer, C. Calle, A. Schweiger, H. Schönberg and H. Grützmacher, *Science*, 2005, **307**, 235–238; (d) P. Chaudhuri and K. Wieghardt, *Prog. Inorg. Chem.*, 2001, **50**, 151; (e) S. Kimura, E. Bill, E. Bothe, T. Weyhermüller and K. Wieghardt, *J. Am. Chem. Soc.*, 2001, **123**, 6025; (f) F. N. Penkert, T. Weyhermüller, E. Bill, P. Hildebrandt, S. Lecomte and K. Wieghardt, *J. Am. Chem. Soc.*, 2000, **122**, 9663–9673.

7 (a) J. C. Pessoa, S. Etcheverry and D. Gambino, *Coord. Chem. Rev.*, 2015, **301-302**, 24–48; (b) D. Rehder, *Future Med. Chem.*, 2012, **4**, 1823–1837; (c) D. C. Crans and T. J. Meade, *Inorg. Chem.*, 2013, **52**, 12181–12183; (d) D. C. Crans, K. A. Woll, K. Prusinskas, M. D. Johnson and E. Norkus, *Inorg. Chem.*, 2013, **52**, 12262–12275; (e) C. J. Schneider, G. Zampella, L. DeGioa and V. L. Pecoraro, in *ACS Symposium Series, vol. 974: Vanadium: The Versatile Metal*, ed. K. Kustin, J. C. Pessoa and D. C. Crans, American Chemical Society, Washington, DC, 2009, ch. 12, pp. 148–162.

8 (a) M. Stylianou, C. Drouza, J. Giapintzakis, G. I. Athanasopoulos and A. D. Keramidas, *Inorg. Chem.*, 2015, **54**, 7218–7229; (b) S. Ghorai and C. Mukherjee, *Chem. Commun.*, 2012, **48**, 10180–10182; (c) A. Saha Roy, P. Saha, N. Das Adhikary and P. Ghosh, *Inorg. Chem.*, 2011, **50**, 2488–2500; (d) C. Drouza and A. D. Keramidas, *Inorg. Chem.*, 2008, **47**, 7211–7224.

9 (a) M. Shit, S. Bera, S. Maity, S. Maji, T. Weyhermüller and P. Ghosh, *Eur. J. Inorg. Chem.*, 2016, 330–338; (b) S. Kundu, S. Maity, T. Weyhermüller and P. Ghosh, *Inorg. Chem.*, 2013, **52**, 7417–7430; (c) S. Kundu, S. Maity, A. N. Maity, S.-C. Ke and P. Ghosh, *Dalton Trans.*, 2013, **42**, 4586–4601.

10 (a) A. Padmaja, K. Laxmi and Ch. S. Devi, *J. Indian Chem. Soc.*, 2011, **88**, 183–187; (b) R. A. Rowe and M. M. Jones, *Inorg. Synth.*, 1957, **5**, 113–115.

11 (a) J. Chakravarty, S. Dutta, S. K. Chandra, P. Basu and A. Chakravorty, *Inorg. Chem.*, 1993, **32**, 4249–4255; (b) J. Chakravarty, S. Dutta, A. Dey and A. Chakravorty, *J. Chem. Soc., Dalton Trans.*, 1994, 557–561.

12 (a) M. M. Hänninen, A. Peuronen, P. Damlin, V. Tyystjärvi, H. Kiveläc and A. Lehtonen, *Dalton Trans.*, 2014, **43**, 14022–14028; (b) O. Wichmann, H. Sopo, A. Lehtonen and R. Sillanpää, *Eur. J. Inorg. Chem.*, 2011, 1283–1291; (c) C. Drouza, V. Tolis, V. Gramlich, C. Raptopoulou, A. Terzis, M. P. Sigalas, T. A. Kabanos and A. D. Keramidas, *Chem. Commun.*, 2002, 2786–2787.

13 (a) S. P. Rath, K. K. Rajak and A. Chakravorty, *Inorg. Chem.*, 1999, **38**, 4376–4377; (b) B. Baruah, S. Das and A. Chakravorty, *Inorg. Chem.*, 2002, **41**, 4502–4508.

14 5: a (Å) = 11.4498(12), b (Å) = 12.7287(13), c (Å) = 22.167(2), $α$ (deg) = 90.884(7), $β$ (deg) = 96.569(7), $γ$ (deg) = 102.967(6) and V = 3124.8(6), space group, $P\bar{1}$.

15 P. B. Chatterjee, O. G. Zapata, L. L. Quinn, G. Hou, H. Hamaed, R. W. Schurko, T. Polenova and D. C. Crans, *Inorg. Chem.*, 2011, **50**, 9794–9803.

16 (a) S. Ghorai, A. Sarmah, R. K. Roy, A. Tiwari and C. Mukherjee, *Inorg. Chem.*, 2016, **55**, 1370–1380; (b) A. V. Piskunov, I. V. Ershova, A. S. Bogomyakov, A. G. Starikov, G. K. Fukin and V. K. Cherkasov, *Inorg. Chem.*, 2015, **54**, 6090–6099;

(c) M. K. Mondal, A. K. Biswas, B. Ganguly and C. Mukherjee, *Dalton Trans.*, 2015, **44**, 9375–9381; (d) A. V. Piskunov, I. N. Meshcheryakova, I. V. Ershova, A. S. Bogomyakov, A. V. Cherkasov and G. K. Fukin, *RSC Adv.*, 2014, **4**, 42494–42505; (e) R. Rakshit, S. Ghorai, S. Biswas and C. Mukherjee, *Inorg. Chem.*, 2014, **53**, 3333–3337; (f) A. Rajput, A. K. Sharma, S. K. Barman, D. Koley, M. Steinert and R. Mukherjee, *Inorg. Chem.*, 2014, **53**, 36–48; (g) S. Hananouchi, B. T. Krull, J. W. Ziller, F. Furche and A. F. Heyduk, *Dalton Trans.*, 2014, **43**, 17991–18000; (h) M. M. Hänninen, P. Paturi, H. M. Tuononen, R. Sillanpää and A. Lehtonen, *Inorg. Chem.*, 2013, **52**, 5714–5721; (i) W. Kaim, *Inorg. Chem.*, 2011, **50**, 9752–9765; (j) C. Mukherjee, T. Weyhermüller, E. Bothe and P. Chaudhuri, *Inorg. Chem.*, 2008, **47**, 11620–11632; (k) P. Chaudhuri, C. N. Verani, E. Bill, E. Bothe, T. Weyhermüller and K. Wieghardt, *J. Am. Chem. Soc.*, 2001, **123**, 2213–2223.

17 (a) S. Mondal, P. Ghosh and A. Chakravorty, *Inorg. Chem.*, 1997, **36**, 59–63; (b) S. Dutta, S. Mondal and A. Chakravorty, *Polyhedron*, 1995, **14**, 1163–1168; (c) S. Mondal, S. Dutta and A. Chakravorty, *Dalton Trans.*, 1995, 1115–1120; (d) P. B. Chatterjee, S. Bhattacharya, A. Audhya, K.-Y. Choi, A. Endo and M. Chaudhury, *Inorg. Chem.*, 2008, **47**, 4891–4902; (e) S. K. Dutta, S. Samanta, D. Ghosh, R. J. Butcher and M. Chaudhury, *Inorg. Chem.*, 2002, **41**, 5555–5560; (f) P. B. Chatterjee, N. Kundu, S. Bhattacharya, K.-Y. Choi, A. Endo and M. Chaudhury, *Inorg. Chem.*, 2007, **46**, 5483–5485; (g) M. R. Maurya, S. Agarwal, C. Bader, M. Ebel and D. Rehder, *Dalton Trans.*, 2005, 537–544; (h) M. Farahbakhsh, H. Schmidt and D. Rehder, *Chem. Commun.*, 1998, 2009–2010; (i) B. Biswas, T. Weyhermüller, E. Bill and P. Chaudhuri, *Inorg. Chem.*, 2009, **48**, 1524–1532; (j) C. R. Cornman, G. J. Colpas, J. D. Hoeschele, J. Kampf and V. L. Pecoraro, *J. Am. Chem. Soc.*, 1992, **114**, 9925–9933; (k) S. R. Cooper, Y. B. Koh and K. N. Raymond, *J. Am. Chem. Soc.*, 1982, **104**, 5092–5102.

18 (a) C. Wolff, A. Gottschlich, J. England, K. Wieghardt, W. Saak, D. Haase and R. Beckhaus, *Inorg. Chem.*, 2015, **54**, 4811–4820; (b) C. C. Scarborough and K. Wieghardt, *Inorg. Chem.*, 2011, **50**, 9773–9793; (c) E. Gore-Randall, M. Irwin, M. S. Denning and J. M. Goicoechea, *Inorg. Chem.*, 2009, **48**, 8304.

19 (a) T. Onishi, Y. Takano, Y. Kitagawa, T. Kawakami, Y. Yoshioka and K. Yamaguchi, *Polyhedron*, 2001, **20**, 1177–1184; (b) H. Nagao, M. Nishino, Y. Shigeta, T. Soda, Y. Kitagawa, T. Onishi, Y. Yoshioka and K. Yamaguchi, *Coord. Chem. Rev.*, 2000, **198**, 265–295; (c) M. Mitani, H. Mori, Y. Takano, D. Yamaki, Y. Yoshiok and K. Yamaguchi, *J. Chem. Phys.*, 2000, **113**, 4035–4051.

20 (a) G. M. Sheldrick, *ShelXS97*, Universitat Gottingen, Gottingen, Germany, 1997; (b) G. M. Sheldrick, *ShelXL97*, Universitat Gottingen, Gottingen, Germany, 1997; (c) G. M. Sheldrick, *XS. Version 2013/1*, Georg-August-Universitat Gottingen, Gottingen, Germany, 2013; (d) G. M. Sheldrick, *Acta Crystallogr., Sect. A: Found. Adv.*, 2015, **71**, 3–8; (e) G. M. Sheldrick, *Acta Crystallogr., Sect. C: Struct. Chem.*, 2015, **71**, 3–8; (f) A. L. Spek, *Acta Crystallogr., Sect. D: Biol. Crystallogr.*, 2009, **65**, 148–155;

(g) A. L. Spek, Platon – A Multipurpose Crystallographic Tool, Utrecht University, Utrecht, The Netherlands, 2011.

21 M. J. Frisch, G. W. Trucks, H. B. Schlegel, G. E. Scuseria, M. A. Robb, J. R. Cheeseman Jr., J. A. Montgomery, T. Vreven, K. N. Kudin, J. C. Burant, J. M. Millam, S. S. Iyengar, J. Tomasi, V. Barone, B. Mennucci, M. Cossi, G. Scalmani, N. Rega, G. A. Petersson, H. Nakatsuji, M. Hada, M. Ehara, K. Toyota, R. Fukuda, J. Hasegawa, M. Ishida, T. Nakajima, Y. Honda, O. Kitao, H. Nakai, M. Klene, X. Li, J. E. Knox, H. P. Hratchian, J. B. Cross, V. Bakken, C. Adamo, J. Jaramillo, R. Gomperts, R. E. Stratmann, O. Yazyev, J. A. Austin, R. Cammi, C. Pomelli, J. W. Ochterski, P. Y. Ayala, K. Morokuma, G. A. Voth, P. Salvador, J. J. Dannenberg, V. G. Zakrzewski, S. Dapprich, A. D. Daniels, M. C. Strain, O. Farkas, D. K. Malick, A. D. Rabuck, K. Raghavachari, J. B. Foresman, J. V. Ortiz, Q. Cui, A. G. Baboul, S. Clifford, J. Cioslowski, B. B. Stefanov, G. Liu, A. Liashenko, P. Piskorz, I. Komaromi, R. L. Martin, D. J. Fox, T. Keith, M. A. Al-Laham, C. Y. Peng, A. Nanayakkara, M. Challacombe, P. M. W. Gill, B. Johnson, W. Chen, M. W. Wong, C. Gonzalez and J. A. Pople, *GAUSSIAN 03 (Revision E.01)*, Gaussian, Inc., Wallingford, CT, 2004.

22 (a) R. G. Parr and W. Yang, *Density Functional Theory of Atoms and Molecules*, Oxford University Press, Oxford, UK, 1989; (b) D. R. Salahub and M. C. Zerner, *The Challenge of d and f Electrons, ACS Symposium Series 394*, American Chemical Society, Washington, DC, 1989; (c) W. Kohn and L. J. Sham, *Phys. Rev.*, 1965, **140**, A1133–A1138; (d) P. Hohenberg and W. Kohn, *Phys. Rev.*, 1964, **136**, B864–B871.

23 (a) R. E. Stratmann, G. E. Scuseria and M. Frisch, *J. Chem. Phys.*, 1998, **109**, 8218–8224; (b) M. E. Casida, C. Jamoroski, K. C. Casida and D. R. Salahub, *J. Chem. Phys.*, 1998, **108**, 4439–4449; (c) R. Bauernschmitt, M. Haser, O. Treutler and R. Ahlrichs, *Chem. Phys. Lett.*, 1996, **256**, 454–464.

24 (a) A. D. Becke, *J. Chem. Phys.*, 1993, **98**, 5648–5652; (b) B. Miehlich, A. Savin, H. Stoll and H. Preuss, *Chem. Phys. Lett.*, 1989, **157**, 200–205; (c) C. Lee, W. Yang and R. G. Parr, *Phys. Rev. B: Condens. Matter Mater. Phys.*, 1988, **37**, 785–789.

25 P. Pulay, *J. Comput. Chem.*, 1982, **3**, 556.

26 H. B. Schlegel and J. J. McDouall, in *Computational Advances in Organic Chemistry*, ed. C. Ogretir and I. G. Csizmadia, Kluwer Academic, The Netherlands, 1991, pp. 167–185.

27 (a) P. J. Hay and W. R. Wadt, *J. Chem. Phys.*, 1985, **82**, 270–283; (b) W. R. Wadt and P. J. Hay, *J. Chem. Phys.*, 1985, **82**, 284–298; (c) P. J. Hayand and W. R. Wadt, *J. Chem. Phys.*, 1985, **82**, 299–310.

28 W. J. Hehre, R. Ditchfield and J. A. Pople, *J. Chem. Phys.*, 1972, **56**, 2257–2261.

29 (a) V. A. Rassolov, M. A. Ratner, J. A. Pople, P. C. Redfern and L. A. Curtiss, *J. Comput. Chem.*, 2001, **22**, 976–984; (b) M. M. Francl, W. J. Pietro, W. J. Hehre, J. S. Binkley, D. J. DeFrees, J. A. Pople and M. S. Gordon, *J. Chem. Phys.*, 1982, **77**, 3654–3665; (c) P. C. Hariharan and J. A. Pople, *Mol. Phys.*, 1974, **27**, 209–214; (d) P. C. Hariharan and J. A. Pople, *Theor. Chim. Acta*, 1973, **28**, 213–222; (e) W. J. Hehre, R. Ditchfield and J. A. Pople, *J. Chem. Phys.*, 1972, **56**, 2257–2261.